The Relationship between Opsin Overexpression and Photoreceptor Degeneration

Elaine Tan,[1,2] *Quan Wang,*[3] *Alexander B. Quiambao,*[1] *Xiaoping Xu,*[2,4] *Nasser M. Qtaishat,*[1] *Neal S. Peachey,*[2,4,5] *Janis Lem,*[6] *Steven J. Fliesler,*[7] *David R. Pepperberg,*[1] *Muna I. Naash,*[1] *and Muayyad R. Al-Ubaidi*[1,3]

Purpose. To characterize the process by which overexpression of normal opsin leads to photoreceptor degeneration.

Methods. Three transgenic mouse lines were generated that express different levels of an opsin with three amino acid modifications at the C terminus. These modifications created an epitopic site that can be readily distinguished from the endogenous protein using a bovine opsin-specific antibody. Evidence of degeneration associated with opsin overexpression was provided by anatomic studies and electroretinogram (ERG) recordings. Western blot analysis was used to confirm the production of the transgenic opsin, and an enzyme-linked immunosorbent assay (ELISA) was used to determine the amounts of opsin overexpressed in each line. Immunocytochemistry was used to determine the cellular localization of transgenic opsin. Amounts of 11-*cis* retinal were determined by extraction and high-performance liquid chromatography (HPLC).

Results. Opsin expression levels in the three lines were found to be 123%, 169%, and 222% of the level measured in nontransgenic animals, providing direct correlation between the level of transgene expression and the severity of the degenerative phenotype. In the lower expressing lines, ERG a-wave amplitudes were reduced to less than approximately 30% and 15% of normal values, whereas responses of the highest expressing line were indistinguishable from noise. In the lowest expressor, a 26% elevation in 11-*cis* retinal was observed, whereas in the medium and the high expressors, 11-*cis* retinal levels were increased by only 30% to 33%, well below the 69% and 122% increases in opsin levels.

Conclusions. The overexpression of normal opsin induces photoreceptor degeneration that is similar to that seen in many mouse models of retinitis pigmentosa. This degeneration can be induced by opsin levels that exceed by only approximately 23% that of the normal mouse retina. Opsin overexpression has potential implications in retinitis pigmentosa. (*Invest Ophthalmol Vis Sci.* 2001;42:589–600)

From the [1]Department of Ophthalmology and Visual Sciences, College of Medicine, and the [3]Department of Biological Sciences, College of Liberal Arts and Sciences, University of Illinois at Chicago; the [2]Research Service, Hines VA Hospital, Illinois; Departments of [4]Neurology and [5]Ophthalmology, Stritch School of Medicine, Loyola University of Chicago, Maywood, Illinois; the [6]Department of Ophthalmology, New England Eye Center, Boston, Massachusetts; and [7]Saint Louis University Eye Institute and the Cell and Molecular Biology Graduate Program, Saint Louis University School of Medicine, Missouri.

Supported by Grants EY11376, EY01792, EY05494, and EY06045 from the National Eye Institute; the Department of Veterans Affairs; the Illinois Eye Fund; and an unrestricted departmental grant from Research to Prevent Blindness.

Submitted for publication August 7, 2000; revised October 30, 2000; accepted November 15, 2000.

Commercial relationships policy: N.

Corresponding author: Muayyad R. Al-Ubaidi, Department of Cell Biology, University of Oklahoma Health Sciences Center, 940 Stanton L. Young Boulevard, BMSB 781, Oklahoma City, OK 73104.
muayyad-al-ubaidi@ouhsc.edu

More than 90 mutations in the rhodopsin gene have been found to be associated with retinitis pigmentosa,[1] a heterogeneous set of diseases characterized by night blindness and progressive loss of peripheral vision resulting from rod photoreceptor degeneration.[2–5] A number of transgenic mouse models carrying different mutant opsins have been established to confirm a causal relationship between the mutations and the disease phenotype, as well as to determine the mechanism by which a mutation may trigger photoreceptor degeneration.[6–12] However, results from recent studies in which mice expressing normal human,[10] mouse,[11] or pig[13] opsin transgenes as control experiments have raised questions about the validity of using transgenic mouse models expressing mutant opsins to study retinal degeneration. Overexpression of normal opsin leads to a degenerative phenotype indistinguishable from that observed in mice expressing mutant forms of opsin.[7–12,14] When the ratio of transgene transcript to that of endogenous protein is between 0.1 and 0.3, the degeneration is slow and mice retain more than 50% of their photoreceptors by 8 weeks of age.[11] However, when the ratio is higher the severity of the degeneration increases accordingly.[11] These data reflect the tight regulation of the opsin gene and the detrimental effects of increased levels of expression.[11] In another study, expression of normal human opsin at a ratio of unity relative to endogenous opsin does not cause retinal degeneration, whereas an increase of fivefold causes severe retinal degeneration.[10] The observation that photoreceptor degeneration occurs at a rate dependent on the steady state levels of opsin mRNA[10,11] suggests that the total amount of opsin expressed in the photoreceptor cell may play a key role in triggering photoreceptor cell death.

Although photoreceptor degeneration resulting from opsin overexpression has been described, no characterization of the pattern and rate of the associated degeneration or the possible mechanism leading to the degeneration has been provided. In the present study, we investigated the correlation between the amount of opsin expressed and the rate of retinal degeneration. Furthermore, we investigated the mechanism through which overexpression of opsin can lead to photoreceptor cell death. To accomplish these goals, we used a transgene construct in which three amino acid substitutions were made at the C terminus to give the transgene bovine opsin-specific immunoreactivity. We refer to this as the *Bouse* (bovine and mouse) opsin transgenic construct. These substitutions, which have not been associated with any retinal disease, allowed the transgenic protein to be distinguished within the environment of the endogenous protein using the bovine opsin-specific monoclonal antibody (mAb) 3A6.[15,16]

Three transgenic mouse lines designated *Bouse A, Bouse B,* and *Bouse C,* were established from the injection of the *Bouse* opsin transgenic construct. Retinas of *Bouse* transgenic mice were examined at specific ages with electroretinography to define the functional competence of the retina, with immunocytochemistry to determine the cellular localization of transgenic opsin, and enzyme-linked immunosorbent assay (ELISA) to determine the opsin expression levels. The results confirm that the severity of degeneration depends on the level of opsin

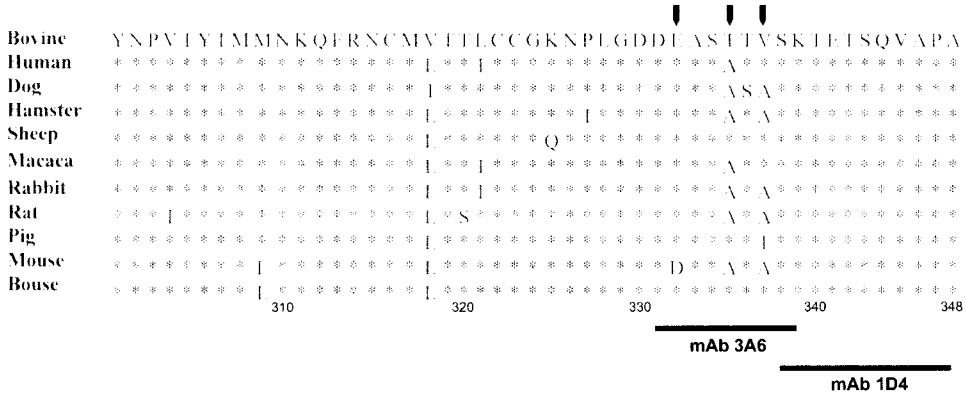

FIGURE 1. Alignment of bovine, human, dog, hamster, sheep, *Macaca*, rabbit, rat, pig, and mouse opsins from amino acids 301 to 348, with the amino acid sequence for the *Bouse* transgene shown last. *Asterisks*: similar amino acids; *single letters*: abbreviations for different amino acids; *arrows*: the three amino acids modified in *Bouse*. The recognition epitopes for mAbs 3A6 and 1D4 are shown as the *solid lines* under the sequence.

expression and demonstrates that an approximate 23% overexpression of opsin is sufficient to trigger photoreceptor degeneration.

MATERIALS AND METHODS

Construction of the Transgene

The *Bouse* transgenic construct was prepared from a 15-kb mouse genomic fragment containing the entire mouse opsin gene including 6 kb of the 5′ flanking sequence, all exons and introns, and 3 kb of the 3′ flanking sequence.[17] The C-terminal modifications were introduced using polymerase chain reaction (PCR) site-directed mutagenesis.[8] These modifications, which generated two restriction fragment length polymorphisms (RFLPs) by eliminating a *Bsa*HI restriction site and creating a *Stu*I restriction site, allowed the transgene product to be easily distinguished from endogenous opsin at the DNA level. Subsequent sequence analysis was performed to ensure that no unintended changes were introduced. The construct was digested with *Sal*I to release the 15-kb fragment and then electrophoresed through a 1% agarose gel. The DNA fragment of interest was electroeluted, precipitated, and purified through a desalting column (Elu-tip; Schleicher & Schuell, Keene, NH).

As shown in Figure 1, there are only three amino acid differences (D332E, A335T, and A337V) between mouse and bovine rhodopsin at the epitopic site recognized by mAb 3A6. Although the C terminus has been demonstrated to be crucial for the proper functioning of the molecule,[18] these specific amino acids are not involved in any known function or associated with photoreceptor degeneration.

Generation of Transgenic Mice and Screening of Potential Founders

Transgenic mice were produced using established protocols,[19] where the 15-kb *Sal*I fragment of the *Bouse* construct (at 1 μg/ml in 10 mM Tris, 0.1 mM EDTA [pH 8.0]) was injected into single-cell mouse embryos. Potential transgenic founders (F_0) and their offspring (F_1 and later) were identified by PCR.[20] DNA was extracted from ear punches and used as the template for an amplification reaction in the presence of a mouse opsin-specific primer (MRA 225: AAAGCAGGCTGTGAAGCACACTGC) and a transgene-specific primer (MRA 226: GTCTTGGAAACGGTGGTAGAGGCC). *Bouse* potential founder mice were mated to breeders (an in-house inbred strain produced from a cross between FVB/N and C57BL/6 mice) to produce the first generation (F_1) and, subsequently, the mice used here. The *rd* mutation present in the FVB/N background was bred out, and the line was maintained by continuous inbreeding.[21,22]

Southern blot analysis was used to determine the pattern of transgene integration and copy number in the three transgenic lines. Genomic DNA was isolated from tail clippings by use of a kit (QIAamp Tissue Kit; Qiagen, Valencia, CA). A 30-μg DNA aliquot extracted from each animal was digested with *Bam*HI at 37°C overnight, electrophoresed in a 0.8% Tris-acetate agarose gel, and transferred onto a membrane (Nytran Plus; Schleicher & Schuell). A 4-kb P^{32}-labeled *Eco*RI-*Sal*I fragment of the 3′ flanking sequences of the mouse opsin gene was used as a probe.[17] This probe labels the endogenous opsin gene as well as the integrated transgene. By labeling the junction between the transgene and the surrounding DNA, this probe allowed the differentiation between the endogenous gene and the junctional fragment of the transgene. Hybridization and wash conditions were as described previously.[23] Comparative densitometric measurements of the transgene and endogenous specific bands were used to determine the transgene copy numbers.

To express the *Bouse* transgene in the absence of endogenous opsin, *Bouse* B transgenic mice were mated to mice with targeted disruption of the opsin gene ($opsin^{-/-}$), and the offspring were screened for the presence of the transgene (as described earlier) and the knockout construct.[24,25] Animals that were heterozygous for both *Bouse* and the knockout mutation (i.e., $opsin^{+/-}$) were mated to $opsin^{-/-}$ mice to produce animals that are heterozygous for *Bouse* and $opsin^{-/-}$.

All experiments were approved by the local Institutional Animal Care and Use Committees and conformed to the National Institutes of Health Guide for the Care and Use of Laboratory Animals and the ARVO Statement for the Use of Animals in Ophthalmic and Vision Research.

Electroretinography

ERGs were recorded from the corneal surface of mice, as described previously.[22] In brief, after overnight dark adaptation, mice were anesthetized with ketamine (80 mg/kg) and xylazine (16 mg/kg) and placed on a heating pad after the pupils were dilated (1% tropicamide; 2.5% phenylephrine HCl). Responses were amplified (1–1000 Hz), averaged, and stored using a signal-averaging system (Compact 4; Nicolet, Madison, WI). Strobe flash stimuli were presented in a Ganzfeld (Nicolet), first in the dark and then superimposed on a steady rod-desensitizing adapting field (1.3 log candelas [cd]/m^2), after a 7-minute interval was allowed for light adaptation.[26] Flash intensities were controlled with neutral density filters (Wratten 96; Kodak, Rochester, NY) and ranged from −3.0 to 1.0 log cd sec/m^2, calibrated with a photometer (model 550; EG&G, Gaithersburg, MD).

Histology and Morphometry

The morphologic appearance of the transgenic and normal retinas was examined after fixation in mixed aldehyde fixative and tissue processing, as described previously.[27] Sections were examined by microscope (Axioskope; Zeiss, Oberkochen, Germany).

For morphometric analysis, digital images of retinal cross sections were captured with a microscope (Olympus, Lake Success, NY) fitted with a digital camera (Sensus; Photometrics, Tucson, AZ). Photoreceptor nuclei were counted in a microscopic field that spanned 100 μm and was centered 300 μm from the edge of the optic nerve head. The 100-μm field was determined by an imaging system (MetaMorph; Universal Imaging, West Chester, PA). This measurement was performed on both sides of the optic nerve head for each section. No

differences were found in the number of photoreceptor nuclei between these regions. Three sections from each of three retinas were examined for each time point.

Light Microscopic Immunocytochemistry

Immunocytochemical analysis was performed after a 4- to 16-hour fixation of enucleated eyes in Davidson fixative[28,29] and subsequent removal of the anterior segment. Tissues were cryoprotected with 30% sucrose in phosphate-buffered saline (PBS; 140 mM NaCl, 2.7 mM KCl, 10 mM Na_2HPO_4, and 1.76 mM KH_2PO_4), embedded in optimal cutting temperature compound (OCT; Miles Diagnostics, Elkhart, IN), and snap frozen in an isopentane-dry ice bath. Six-micrometer sections were cut, picked up on glass slides, and allowed to dry at room temperature. Sections were incubated with PBS containing 5% normal goat serum and 0.1% bovine serum albumin (BSA) for 30 minutes at room temperature. After three washes with PBS, sections were incubated with the primary antibody in PBS containing 5% goat serum, 0.1% BSA, and 140 mM NaCl (mAb 1D4 at 1:100 dilution at 4°C) or 500 mM NaCl (mAb 3A6 at 1:20 dilution at room temperature) overnight. After primary antibody incubation, sections were rinsed in PBS three times. The secondary antibody, fluorescein isothiocyanate (FITC)–conjugated goat anti-mouse (Jackson ImmunoResearch, West Grove, PA), was applied at 1:1000 dilution for 30 minutes at room temperature. Sections were then washed three times with PBS, mounted in medium (H-1000; Vector, Burlingame, CA), and viewed with an epifluorescence microscope (Axioskope; Ziess).

Alternatively, hemisected eyes (anterior segment removed) were fixed in mixed aldehyde fixative (0.1 M sodium phosphate buffer [pH 7.4], containing 2.5% glutaraldehyde, 2.0% paraformaldehyde, and 0.025% $CaCl_2$) and processed for embedding in resin (LR White; Electron Microscopy Sciences, Fort Washington, PA), essentially according to the method of Erickson et al.[30] Thick sections (0.75 μm) were cut with a microtome and placed onto glass slides, followed by treatment for 30 minutes at room temperature with blocking buffer (PBS containing 1% [wt/vol]) radioimmunoassay grade BSA, 10% [vol/vol] normal goat serum, and 0.05% [vol/vol] Triton X-100). Tissue sections were exposed for 2 hours at room temperature, either to rabbit anti-bovine opsin IgG or to nonimmune rabbit serum (each diluted 1:500 with blocking buffer), rinsed briefly with PBS, and treated for 2 hours at room temperature with 1 nm colloidal gold–conjugated goat anti-rabbit IgG secondary antibody (AuroProbe One GAR; Amersham, Arlington Heights, IL; diluted 1:50 [vol/vol] with blocking buffer). Sections were rinsed three times (15 minutes each) with PBS, followed by fixation for 10 minutes at room temperature with 2% (vol/vol) glutaraldehyde in PBS and then rinsed with distilled water (twice, 5 minutes each). Silver intensification was performed with a kit (IntenSE M Silver Enhancement; Amersham), according to the directions of the manufacturer. Sections were then rinsed with distilled water, counterstained with 1% (wt/vol) toluidine blue in 1% (wt/vol) sodium borate, rinsed again with distilled water, air dried, and coverslipped (Permount; Fisher Scientific, Fairlawn, NJ). Sections were viewed and photographed with a photomicroscope (BH-2 with a ×20 DPlanApo objective; Olympus).

Western Blot Analysis

Retinas were isolated, immediately frozen in liquid nitrogen, and stored at −70°C until used. Retinal protein extracts were prepared by homogenization of frozen tissue in PBS containing 1 mM EDTA, 1% Triton X-100, 0.1 mM phenylmethylsulfonyl fluoride (PMSF), and a protease inhibitor cocktail (Mini Complete; Boehringer–Mannheim, Indianapolis, IN). Protein concentrations of the homogenates were determined with a BCA protein assay kit (Pierce, Rockford, IL), using the BSA provided as a calibration standard.

Retinal extracts were combined with Laemmli sample buffer[31] containing 0.2 M Tris (pH 6.8), 1 mM EDTA, 4% (wt/vol) sodium dodecyl sulfate (SDS), 20% (vol/vol) glycerol, 0.005% bromophenol blue, and 5% β-mercaptoethanol. Twenty to 40 μg total protein aliquots of each sample (300 ng from bovine rod outer segment [ROS] extract) were resolved on a 12% SDS–polyacrylamide minigel[31] and transferred[32] to polyvinylidene (PVDF) membrane (Immunoblot; Bio-Rad, Hercules, CA) in a minigel apparatus (Transblot; Bio-Rad) at 200 V for 2 hours in 25 mM Tris, 192 mM glycine, 10% methanol, and 0.1% SDS. Membranes were blocked in 5% nonfat dry milk (Carnation, Glendale, CA) in TTBS (10 mM Tris [pH 7.5], 100 mM NaCl, 0.1% Tween-20) for 1 hour at room temperature with agitation. Primary antibody incubations (mAb 1D4 at 1:3000, mAb 3A6 at 1:1) were performed in 5% milk/TTBS (containing 0.01% Tween-20) for 16 hours, at 4°C for mAb 1D4 and at room temperature for mAb 3A6. Membranes were then washed five times for 5 minutes each at room temperature in TTBS, and incubated in a horseradish peroxidase–linked goat anti-mouse IgG (Pierce) for 1 hour at room temperature, at a dilution of 1:20,000 in 5% milk/TTBS. Membranes were then washed as described earlier. Blots were incubated in an enhanced chemiluminescence detection system (SuperSignal; Pierce) for 5 minutes, and then exposed to film (XAR; Kodak).

Enzyme-Linked Immunosorbent Assay

Protein extracts used for ELISA were prepared from individual animals, as described for Western blot analysis. Control experiments established the linear ranges for total protein loaded, primary and secondary antibody dilutions, and color substrate concentration. Aliquots (5–320 ng total protein from retinal homogenates from mice at postnatal day [P]15) were diluted in PBS for a total sample volume of 50 μl, loaded in duplicates onto a 96-well cell culture dish (Costar, Cambridge, MA), and allowed to bind overnight. Samples were rinsed three times with water, and incubated for 2 hours with blocking buffer (PBS, 0.05% Tween-20, 1 mM EDTA, 0.25% gelatin). Samples were rinsed and allowed to incubate in primary antibody (partially purified mAb 1D4 at 1:1000 and anti-peripherin/rds[33] polyclonal antibody at 1:500, diluted in blocking buffer) for 2 hours. Wells were rinsed as described earlier, blocking buffer was added, incubation was performed for 10 minutes, and the wells were rinsed again. Horseradish peroxidase–labeled secondary antibodies were applied (goat anti-mouse IgG and goat anti-rabbit IgG [Pierce] at a dilution of 1:10,000) in blocking buffer for 2 hours. Samples were rinsed, blocked, and rinsed again as described. Then a 100-μl aliquot of *o*-phenylenediamine substrate (1 mg/ml) in stable peroxide buffer (Pierce) was added to each well and allowed to develop for 30 minutes. The reaction was stopped by adding 50 μl of 2.5 M sulfuric acid to each well, and plates were read at 490 nm (Microplate Autoreader, model EL309; Bio-Tek, Winooski, VT). All steps were performed at room temperature.

The mean optical density readings from blank wells (no protein loaded) were subtracted from readings obtained for the remaining wells. These values were then averaged for duplicate wells. Final values were plotted versus total protein loaded for opsin as well as for peripherin/rds. The slope of the opsin plot (defined by optical density/total protein) was then divided by the slope of the peripherin/rds plot to obtain an opsin/peripherin/rds ratio. Opsin/peripherin/rds ratios from three trials were averaged; values for animals of the same line (i.e., normal and *Bouse* A, B, and C) were then averaged and divided by the mean value obtained for nontransgenic and breeder normal samples to arrive at values for opsin expression levels. The peripherin/rds ratio was used to correct for any degeneration.

Localization of Bouse opsin Anti-Opsin Antibody

ROS membranes were prepared from bovine retinas by discontinuous sucrose density ultracentrifugation, per the method of Papermaster.[34] Purity was assessed by SDS-polyacrylamide gel electrophoresis (SDS-PAGE; broad band at molecular mass 38 kDa, representing 90% of the Coomassie blue–stainable material) and spectral ratio (A_{280}/A_{498} = 1.8–2.0). Rhodopsin was purified from ROS membranes by lectin-affinity column chromatography according to the method of Litman,[35] using concanavalin (ConA)-Sepharose (Sigma, St. Louis, MO), and purity again was assessed by SDS-PAGE and spectral ratio (A_{280}/A_{498} = 1.6). Polyclonal antiserum was raised against purified bovine rhodop-

sin in New Zealand White rabbits, using a standard protocol with adjuvant (Hunter's TitreMax; Sigma). Preimmune serum was obtained before immunization with antigen. A purified IgG fraction of antiserum was obtained by diethylaminoethyl (DEAE) chromatography (Affi-Gel Blue; Bio-Rad), according to the manufacturer's protocol. Titer was assessed to be at least 1:5000 by standard dot blot assay.

Electron Microscopic Immunogold Cytochemistry

Electron microscopic immunogold cytochemistry was performed essentially as described by Erickson et al.[30] Briefly, ultrathin sections (silver-gold) obtained from each of the tissue blocks (embedded in LR White; Electron Microscopy Sciences) were placed onto nickel grids and treated for 15 minutes at room temperature with 50 mM ammonium chloride, followed by blocking for 30 minutes at room temperature with blocking buffer (composition described earlier). Grids were exposed overnight at 4°C, either to rabbit anti-bovine opsin IgG or to nonimmune rabbit serum (each diluted 1:250 with blocking buffer), then rinsed briefly with PBS and treated for 2 hours at room temperature with goat anti-rabbit IgG conjugated to 10 nm colloidal gold (AuroProbe EM GAR G10; Amersham; diluted 1:50 with blocking buffer). After a brief rinsing with PBS, sections were treated with 1% glutaraldehyde (5 minutes at room temperature), rinsed serially with PBS and distilled water, stained with uranyl acetate and lead citrate, rinsed again with distilled water, exposed to OsO_4 vapors, and air dried. Sections were viewed with an electron microscope (JEM-1200EX; JEOL, Tokyo, Japan) at an accelerating voltage of 80 keV.

Retinoid Analysis

Analyses were performed on dark-reared P15 mice. Experiments were performed under dim red light. Each animal was first anesthetized with ketamine (0.15–0.18 mg/g) and xylazine (0.004–0.006 mg/g) and then killed by cervical dislocation. Retinas were removed and then homogenized in 500 μl of PBS supplemented with protease inhibitor cocktail (one tablet protease inhibitor cocktail per 10 ml), using a 1-ml manual tissue grinder (Wheaton, Millville, NJ).

An aliquot (100 μl) of homogenate was added to 200 μl of formaldehyde (37% wt/vol aqueous solution), supplemented with isopropanol and water, and subsequently extracted with *n*-hexane, as previously described.[36] This formaldehyde-based extraction procedure recovers both chromophoric and nonchromophoric 11-*cis* retinal.[37–39] Another 100-μl aliquot of the homogenate was added to 400 μl of isopropanol, supplemented with water, and extracted with *n*-hexane.[36] Levels of 11-*cis* retinal and other retinaldehydes were determined from results obtained with the formaldehyde-based extraction procedure. Data obtained from extractions in the absence of formaldehyde were used to determine levels of retinal.[36] Each sample was then evaporated under nitrogen and redissolved in 200 μl *n*-hexane. Levels of retinoids in each sample were determined by normal-phase high-performance liquid chromatography (HPLC).[36] The last 200-μl aliquot of homogenate was used for protein concentration determination and ELISA.

Results

The microinjection of the *Bouse* construct produced 50 potential founders that were screened for the presence of the transgene in their genome by PCR.[20] Two of these mice (11571 and 11760) were positive for the transgene and when mated to wild-type mice passed the transgene to their offspring in a Mendelian fashion. Southern blot analysis performed on tail DNA extracted from founder animals and members of their offspring showed that founder 11760 had two to four copies of the transgene at a single site of integration. Analysis of transgenic founder 11571 showed that the transgene integrated at two separate sites with two to four copies per site (data not shown). Mating separated these two sites, giving rise to two independent transgenic lines (11571-A and 11571-B). These three lines 11571-A, 11571-B, and 11760, referred to as *Bouse* A, *Bouse* B, and *Bouse* C, respectively, were mated to wild-type mice to generate heterozygous transgenic offspring for analysis.

Electroretinography

To assess retinal function, ERGs were recorded from transgenic mice and nontransgenic littermates. Figure 2A presents dark-adapted ERGs obtained from representative 1-month-old nontransgenic, *Bouse* A, and *Bouse* B mice to flash stimuli that spanned a 4-log-unit range of intensity. At the lowest flash intensity, the response of nontransgenic mice was dominated by the positive-polarity b-wave, reflecting the activity of rod bipolar cells.[40] At the higher flash intensities, the b-wave was preceded by the negative-polarity a-wave, which represents the mass response of the rod photoreceptors.[41] In the transgenic mice, both a- and b-waves were reduced in amplitude at all stimulus intensities. The magnitude of this reduction was greater in *Bouse* B than *Bouse* A mice and was greatest in *Bouse* C mice, in which ERG responses were not distinguishable from the preflash baseline (data not shown). The bottom panels present average intensity–response functions for the major ERG components, a-wave (Fig. 2B) and b-wave (Fig. 2C). In each transgenic line, a- and b-wave amplitudes were well outside the 99% confidence interval defined in nontransgenic mice (dashed lines). The magnitude of this reduction was greatest in *Bouse* C mice and least in *Bouse* A animals. *Bouse* B mice exhibited an intermediate level of amplitude reduction. The amplitude of the cone ERG b-wave was also reduced but to a lesser degree than that seen for the rod ERG (data not shown). This reduction was greatest in *Bouse* C mice and least in *Bouse* A and *Bouse* B animals, implicating a secondary effect on cones of the rod degeneration, as has been seen before in animal models of retinitis pigmentosa[8,10,13,42,43] and in patients with retinitis pigmentosa who have rod-specific gene defects.[44–48]

Retinal Histology in *Bouse* Transgenic Mice

At P10, the histologic appearance of the retina in all three *Bouse* lines was indistinguishable from nontransgenic retinas (Fig. 3). At P30, each transgenic line showed evidence of photoreceptor cell loss that ranged in severity from three to four rows of photoreceptor nuclei in *Bouse* A, to five to six rows in *Bouse* B, to virtually the entire outer nuclear layer (ONL) in *Bouse* C mice. These histologic changes agree well with the ERG recordings made in mice of this age.

Specificity of mAb 3A6

The introduction of three amino acid changes (D332E, A335T, and A337V) at the C terminus of mouse opsin provided an epitope that should be readily recognized by the bovine opsin C-terminus–specific mAb 3A6. Western blot analysis of retinal extracts from P15 nontransgenic and *Bouse* mice confirmed that mAb 3A6 recognized both *Bouse* and bovine opsins, but not the endogenous mouse opsin (Fig. 4B). In comparison, probing with the mammalian opsin-specific mAb 1D4 detected all forms of opsin in both transgenic and nontransgenic retinas (Fig. 4A). Although 1D4 recognized mono- and multimeric forms of opsin, 3A6 detected only the monomeric form (arrows, Fig. 4). Because the same protein samples were used for both blots, it is very likely that the nonrecognition was due to the sensitivity of mAb 3A6 to the secondary structure changes associated with opsin aggregation.

Localization of *Bouse* Opsin

To determine the cellular localization of *Bouse* opsin in the retina, cross sections of P10 transgenic and nontransgenic retinas were immunostained. With mAb 1D4 (Fig. 5, left), staining was restricted to photoreceptors, where the antibody

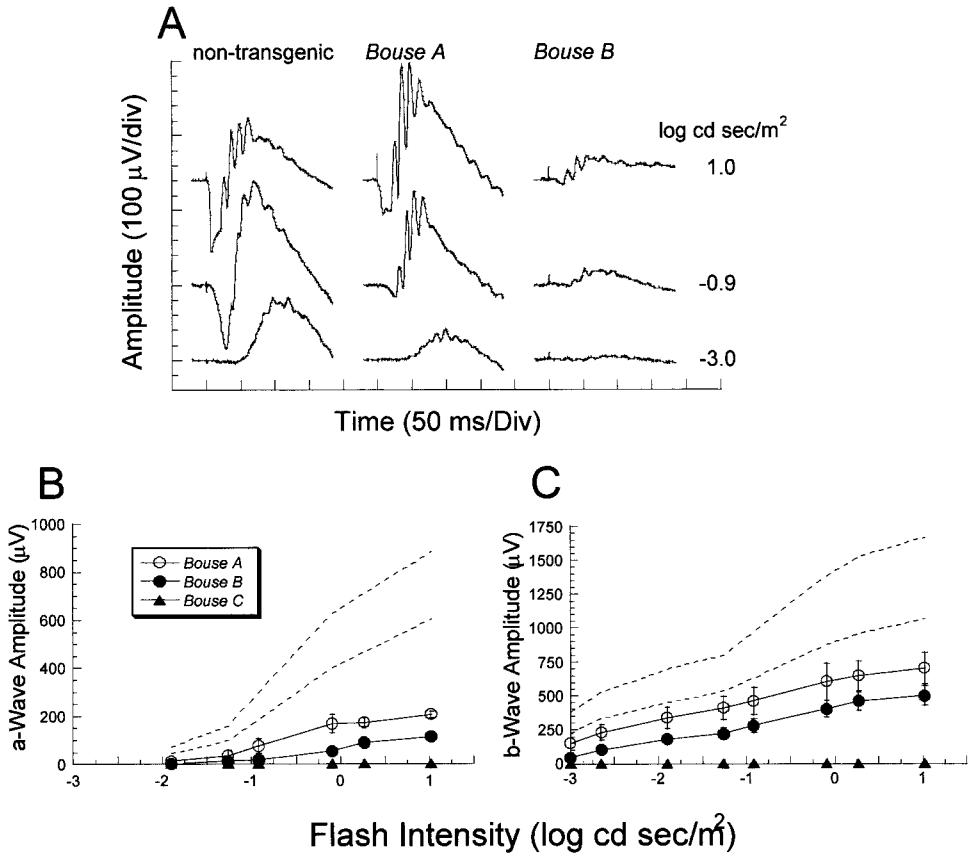

FIGURE 2. Electroretinography of 1-month-old mice. (**A**) Dark-adapted ERG series recorded from nontransgenic, *Bouse* A, and *Bouse* B mice. Stimulus intensities are indicated to the *right*. (**B**) Amplitude of the dark-adapted ERG a-wave plotted as a function of stimulus intensity. (**C**) Intensity–response function for the dark-adapted ERG b-wave. Data points in (**B**) and (**C**) indicate average values. Error bars: ±1 SD; *dashed lines*: 99% confidence interval for results in 25 nontransgenic mice.

labeled outer segments (OSs) most intensely. Under conditions exceeding saturation of the OS epifluorescence signal, moderate labeling of inner segments and photoreceptor cell bodies in the ONL also was observed. A similar staining pattern was seen in nontransgenic animals and in *Bouse* mice. The distribution was similar also when mAb 3A6, which detects *Bouse* opsin, was used, except that only transgenic retinas were stained (Fig. 5, right). This result validates the use of mAb 3A6 to detect the presence of the *Bouse* transgene product against a background of normal mouse opsin.

The localization of opsin (both endogenous and *Bouse*) in transgenic mouse retinas was confirmed independently at the light microscopic level, by using silver-enhanced immunogold labeling (Figs. 6A, 7A), with subsequent subcellular localization by electron microscopic immunogold cytochemistry (Figs. 6B, 6C, 7B, 7C). In this case, a rabbit polyclonal antibody raised

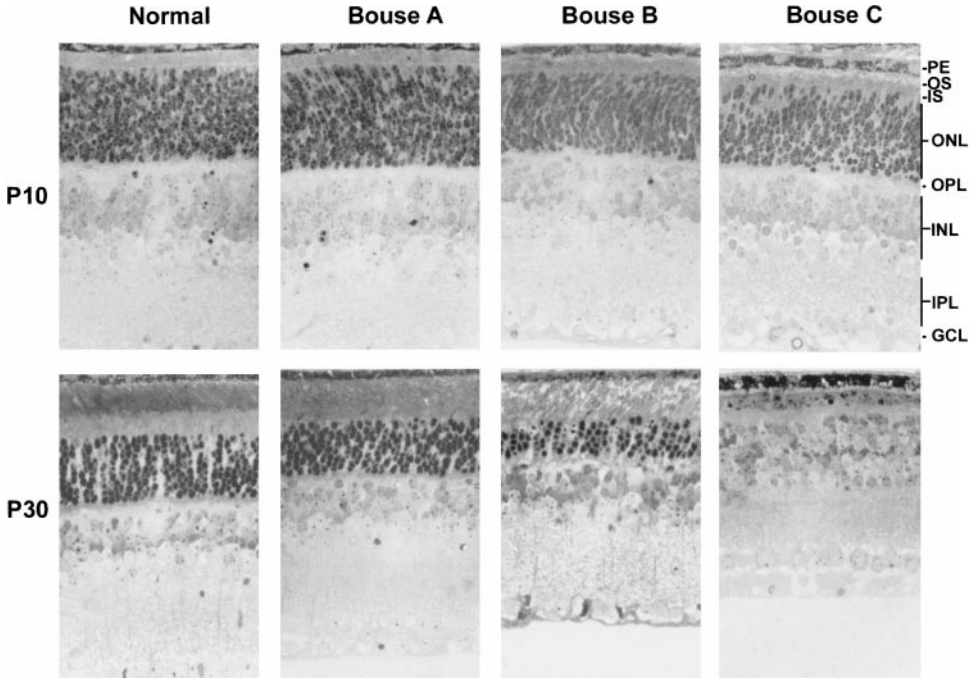

FIGURE 3. Light micrographs of retinal cross sections from cyclic-light–reared nontransgenic mice and age-matched *Bouse* mice at P10 and P30. *Top*: Sections from 10-day-old mice; *bottom*: sections from 1-month-old animals. PE, pigment epithelium; OS, outer segments; IS, inner segments; ONL, outer nuclear layer; OPL, outer plexiform layer; INL, inner nuclear layer; IPL, inner plexiform layer; GCL, ganglion cell layer.

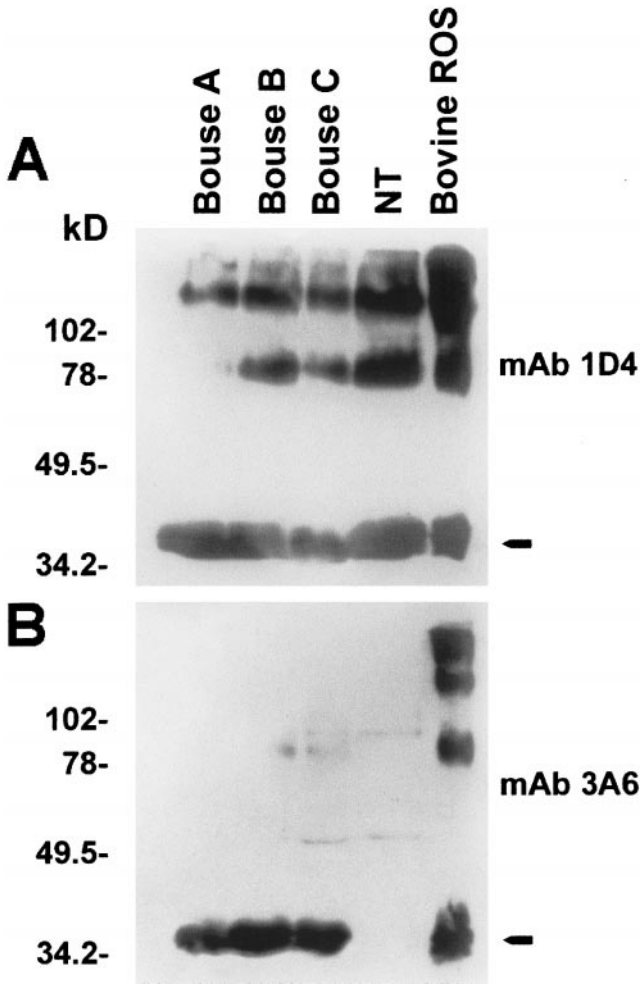

Figure 4. Western blot analysis of *Bouse* opsins at P10. Aliquots of 2 mg protein of extracts from bovine ROS, and nontransgenic (NT) and transgenic retina homogenates were electrophoresed, transferred to PVDF membrane, and probed with mAb 1D4 (1:1000) for detecting opsin contents. Migration of protein molecular weight markers is specified at *left*. *Arrows*: Monomeric form of opsin.

against purified bovine opsin was used, followed by gold-conjugated goat anti-rabbit IgG secondary antibodies for detection. In the retinas of P15 *Bouse* A mice (Fig. 6), opsin was localized almost exclusively to rod photoreceptor OSs. The absence of labeling of some OSs (asterisk, Figs. 6B, 6C) identifies these as cone photoreceptors, because the antibody does not recognize cone opsin (Fliesler SJ, unpublished results, 1997). Vesicular structures were observed at the base of some ROSs (arrowhead, Fig. 6C). However, such structures also were observed with comparable frequency in sections of nontransgenic retinas (not shown). Therefore, these vesicles are not a result of the *Bouse* alteration, but probably represent either misaligned basal discs or a capricious artifact of tissue preparation. Relatively sparse anti-opsin immunolabeling was observed along the rod cell plasmalemma and in other inner segment membrane compartments (Fig. 6C). Even less pronounced immunolabeling was detected at synaptic terminals in the outer plexiform layer (OPL), which was very similar to that observed in nontransgenic retinas and in retinas of *Bouse* B transgenic mice (data not shown). However, in *Bouse* C retinas at P10 (Fig. 7), anti-opsin immunolabeling of photoreceptor cell bodies and in the OPL was considerably more pronounced (Figs. 7A, 7C), reflecting loss of the normally polarized distribution of opsin (i.e., ectopic expression), consistent with the advanced degeneration already present in *Bouse* C retinas at P10. In this case, not only were the OSs very truncated and poorly aligned, but they also had disorganized disc membranes (Fig. 7B).

These results indicate that opsin trafficking and localization in *Bouse* A retinas (and *Bouse* B retinas, not shown) were normal, thus suggesting that defects in opsin transport are unlikely to cause the degeneration noted in these lines. In *Bouse* C, however, the situation was complicated by the severity of degeneration, and it is possible that abnormalities either in opsin transport or in redistribution after initial insertion into the photoreceptor plasma membrane may have accelerated the degenerative process.

Relationship between Severity of Degeneration and Opsin Expression

To determine the level of opsin expression, retinas were examined at P15 by ELISA. When mAb 1D4 was used, the values obtained for total opsin reflect both *Bouse* and endogenous forms. These values were normalized to those obtained for peripherin/rds, a photoreceptor-specific structural protein localized in the OS, using a polyclonal antibody (anti-mRDS-C).[33] Because peripherin/rds is an essential component of the OS,[49,50] this normalization procedure accounted for the loss of OSs due to the degenerative process. As shown in Table 1,

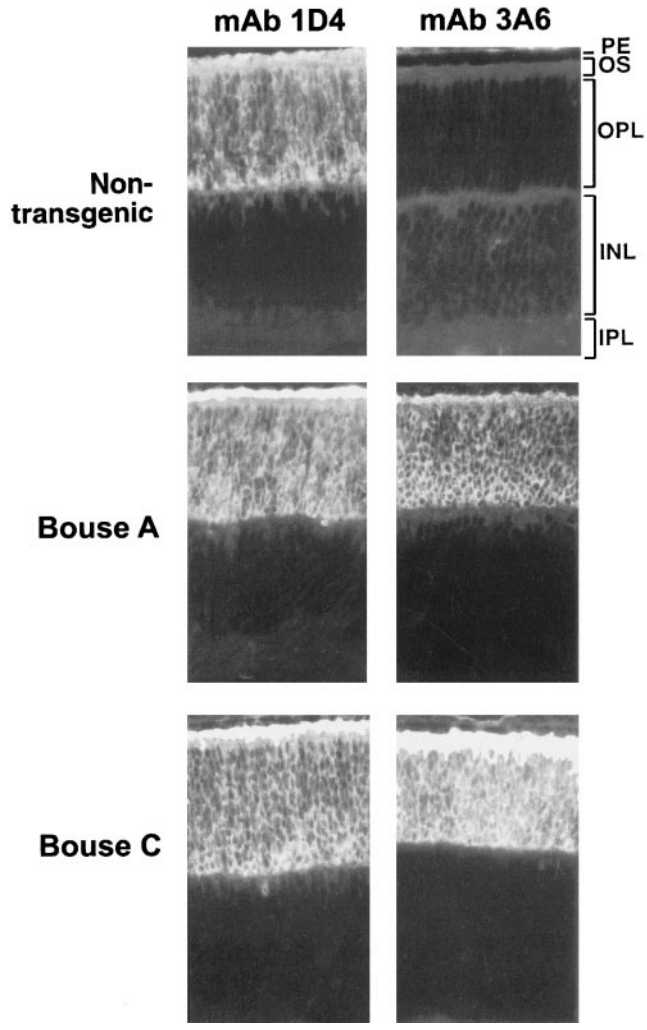

Figure 5. Opsin expression in nontransgenic and P15 *Bouse* A and C retinas. Retina sections of normal and *Bouse* A mice were fixed with Davidson fixative. Anti-opsin mAb 1D4 or 3A6 was applied as the primary antibody for immunostaining. Abbreviations are as in Figure 3.

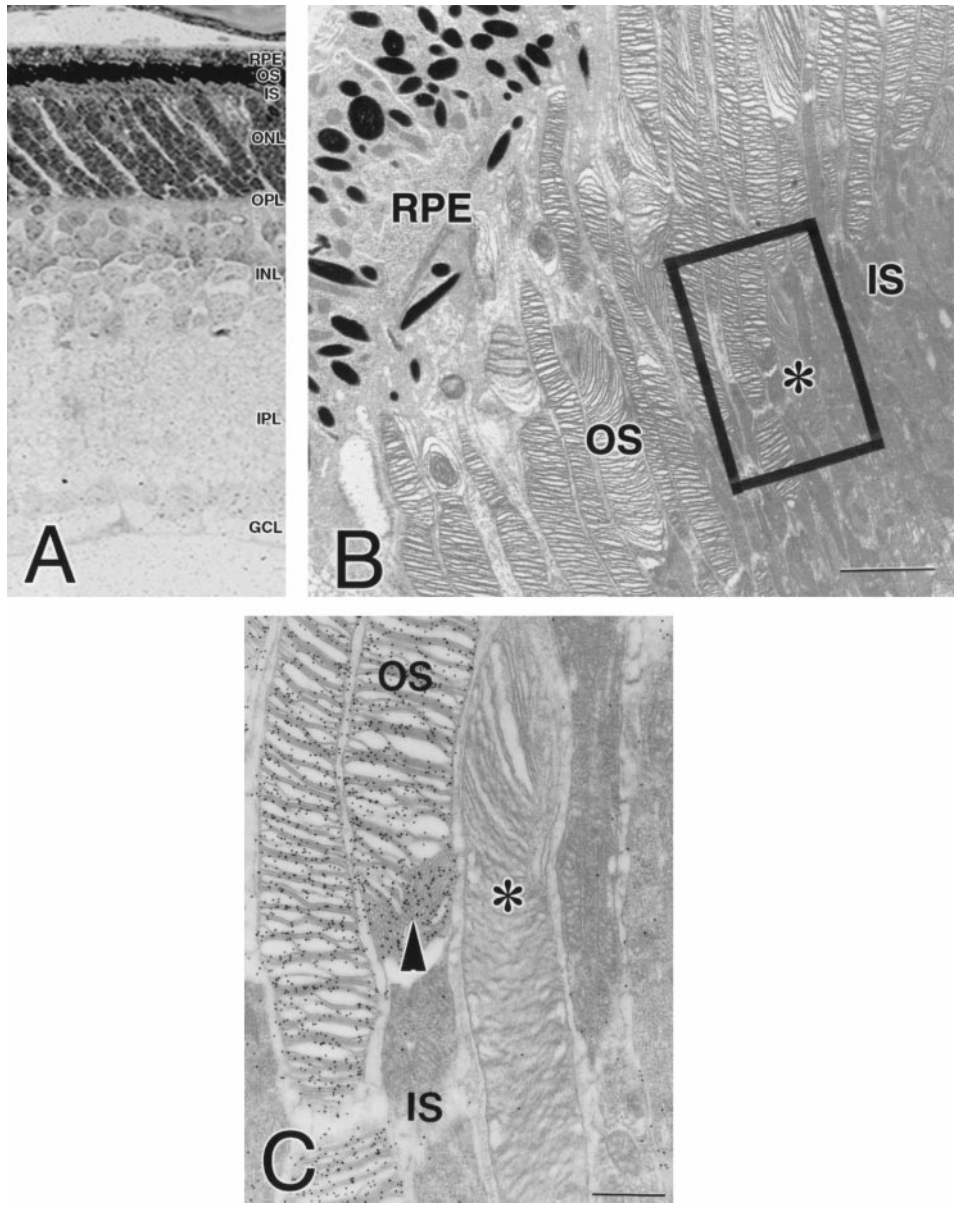

FIGURE 6. Immunogold localization of opsin in P15 *Bouse* A transgenic retina. (**A**) Light microscopic, silver-enhanced immunogold labeling with polyclonal anti-opsin, illustrating restricted localization of opsin to the OS. (**B**) Companion low-magnification electron micrograph, demonstrating normal ultrastructural organization of the *Bouse* A outer retina (RPE–photoreceptor interface). *Rectangle*: Area shown in higher magnification in (**C**). (**C**) Higher magnification electron micrograph, showing immunogold labeling of rod photoreceptors, showing restricted localization of gold label to OS. *Arrowhead*: Vesiculation of basal disc membranes. (✻) Nonlabeled photoreceptor presumed to be a cone. Abbreviations are as in Figure 3. Scale bar, (**B**) 2.5 μm; (**C**) 0.5 μm.

opsin expression levels for *Bouse* A, *Bouse* B, and *Bouse* C mice were found to be, respectively, 123%, 169%, and 222% of the level measured in nontransgenic animals, indicating a correlation between the level of transgene expression and the severity of the degenerative phenotype. Although the *Bouse* A line exhibited the slowest rate of degeneration, these results indicate that overexpression of opsin by approximately 23% is sufficient to trigger photoreceptor cell death, a finding in agreement with that previously reported by Sung et al.[11] This value may not set a lower limit for opsin-induced photoreceptor degeneration, but it clearly demonstrates the sensitivity of rod photoreceptors to opsin overexpression.

11-*cis* Retinal Content of Normal and *Bouse* Retinas

To determine whether an increased level of opsin expression is associated with an increased amount of 11-*cis* retinal, retinas of dark-reared P15 mice were analyzed for the molar quantity of 11-*cis* retinal. Results obtained from nontransgenic and *Bouse* mice (Table 1, middle column) were normalized to the density of photoreceptor nuclei contained in a specified area of the ONL (Table 1, right column). In *Bouse* A mice the 23% elevation, relative to nontransgenic mice, in the amount of opsin was accompanied by an approximately equal increase in the amount of 11-*cis* retinal, (26%). In both *Bouse* B and *Bouse* C mice, however, 11-*cis* retinal levels were increased by only 30% to 33%, well below the 69% and 122% increases in opsin levels found in these two lines. In all animals studied, 11-*cis* retinal was the major retinoid detected in the retina.

Effect of Light on the Rate of Retinal Degeneration

Because the overall amount of rhodopsin in *Bouse* transgenic retinas was increased, the effects of light were investigated. Several litters were reared from birth in constant darkness, and ERG recordings were made at P30, followed by histologic examination. As shown in Figure 8A, the ERGs obtained from *Bouse* A mice were significantly larger when these mice were reared in darkness than when treated under cyclic light ($P < 0.005$, $n = 9$). In comparison, dark rearing had a modest but insignificant benefit in *Bouse* B mice ($P > 0.10$, $n = 8$) and no effect in *Bouse* C animals (Fig. 8A).

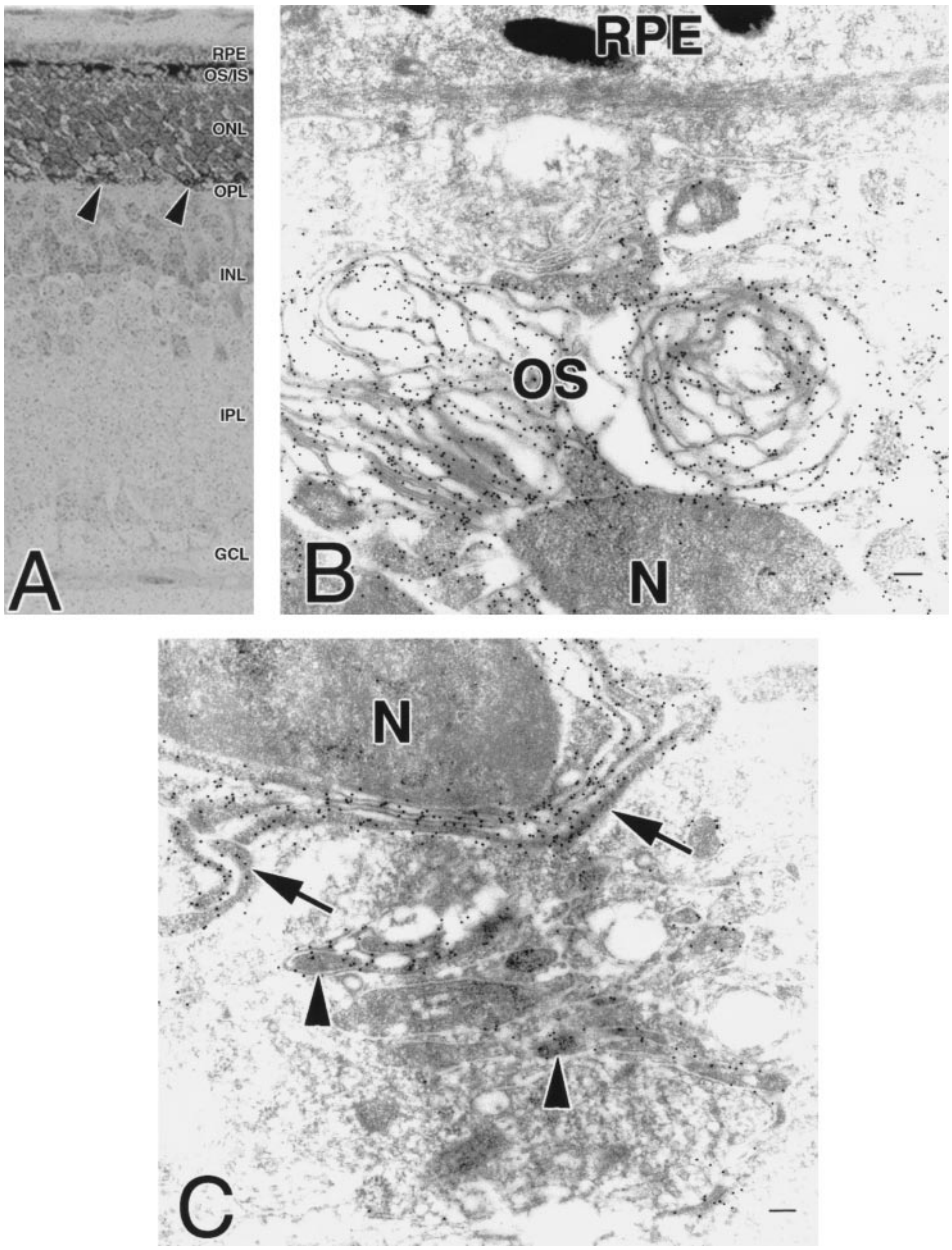

FIGURE 7. Immunogold localization of opsin in P10 *Bouse* C transgenic retina. (**A**) Light microscopic, silver-enhanced immunogold labeling with polyclonal anti-opsin. In addition to the thin, but heavily labeled, OS layer, pronounced ectopic immunolabeling was seen within the ONL and OPL (*arrowheads*). (**B**) Immunogold electron micrograph of outer retina (RPE–photoreceptor interface), showing disorganized, truncated, heavily labeled OS membranes immediately adjacent to a rod cell nucleus (N). (**C**) Immunogold electron micrograph of ONL–OPL interface shows heavy labeling of perinuclear plasma membrane (*arrows*) and other membranous structures (*arrowheads*). Abbreviations are as in Figure 3. Scale bar, (**B**, **C**) 0.5 μm.

Histologic examination of retinas from dark-reared *Bouse* A mice showed improvement consistent with the ERG findings (Fig. 8B). The improvements were most obvious in the appearance of the OSs of dark-reared *Bouse* A mice. However, the histopathologic appearance of the retina from dark-reared *Bouse* B and C mice seemed similar to that of their cyclic light-reared counterparts (data not shown).

TABLE 1. Expression of Opsin and 11-*cis* Retinal in *Bouse* Transgenic Mice

		11-*cis* Retinal	
	OPSIN	**Retina**	**Nuclei**
Nontransgenic	1.00	0.0622 ± 0.005	0.00027 ± 0.000022
Bouse A (n = 7)	1.23 (23)	0.0636 ± 0.005	0.00034 ± 0.000027 (26)
Bouse B (n = 6)	1.69 (69)	0.0638 ± 0.009	0.00035 ± 0.000056 (30)
Bouse C (n = 7)	2.22 (122)	0.0410 ± 0.005	0.00036 ± 0.000041 (33)

Data for opsin reflect the fractional increase in opsin expression relative to that of the nontransgenic (arbitrarily set at unity). Numbers in parentheses indicate percentage over-expression of opsin. 11-*cis* Retinal (in mean nanomoles ± SEM) is expressed per retina and normalized to the number of photoreceptor nuclei (ONL) to account for the degeneration. The data for nontransgenic retinas were obtained from nontransgenic (n = 14) and normal (n = 7) mice.

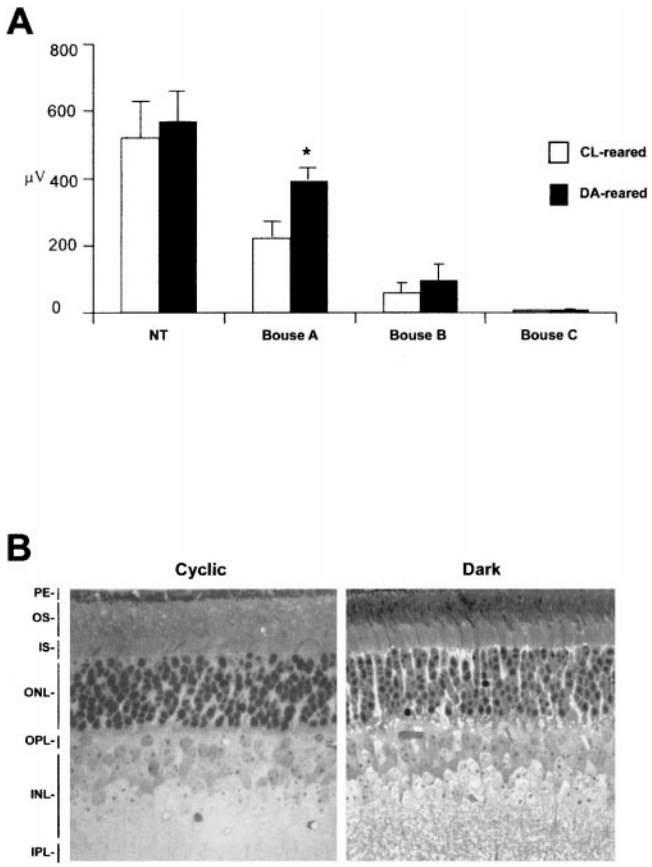

FIGURE 8. (**A**) Amplitude of the dark-adapted ERG a-wave in response to a high-intensity stimulus (1.0 log cd sec/m^2). Data are average results for 5 to 10 mice reared from birth in constant darkness (*filled bars*) or under constant light (*open bars*); error bars: ± 1 SD. (*) Statistically significant differences ($P < 0.05$, *t*-test) between the dark- and cyclic-light–reared group. (**B**) Histologic appearance of cyclic-light– and dark-reared *Bouse* retinas at 30 days of age. Abbreviations are as in Figure 3.

Determining the Effects of the C-Terminal Modifications of *Bouse*

To demonstrate that the C-terminal amino acid alterations made to generate the *Bouse* epitope do not by themselves induce photoreceptor degeneration, *Bouse* mice were bred with opsin$^{-/-}$ mice.[24] Because a minimum of 50% of the wild-type amount of opsin is required to support the morphogenesis of OSs,[24] only *Bouse* B mice were used. After extensive matings, mice that were heterozygous for the *Bouse* B transgene and opsin$^{-/-}$ were obtained. Examination of these animals indicated that their retinal histology and ERG recordings were indistinguishable from those of wild-type mice. As shown in Figure 9, *Bouse* opsin alone supported the OS morphogenesis and maintenance. Dark-adapted ERG a-waves were comparable with those of wild-type mice (data not shown).

DISCUSSION

We generated transgenic mice that express a modified yet normal form of opsin and used these animals to investigate the degenerative process associated with overexpression of opsin. Evidence of photoreceptor degeneration was provided by anatomic and electrophysiological studies of the heterozygous transgenic retina. There was a clear correlation between the severity of the degenerative phenotype and the level of transgene expression. At low levels of expression, however, both transgenic and endogenous opsins were correctly localized to photoreceptor OSs, and opsin was not found in other cellular compartments. This was determined by immunocytochemistry using antibodies that recognize the endogenous mouse opsin (mAb 1D4) or the transgenic *Bouse* form of opsin (mAb 3A6) in which a bovine-like epitope was created by the introduction of three amino acid alterations at the C terminus. Because the *Bouse* transgene did not induce degeneration when expressed in opsin$^{-/-}$ mice (i.e., in the absence of the endogenous opsin) *Bouse* transgenic mice provided an opportunity to examine the implications of rhodopsin overexpression in photoreceptor degeneration.

A number of prior studies have shown that expression of mutant forms of opsins induce photoreceptor degeneration in transgenic mice.[7–12,14] In one study, mice expressing as little as 10% more opsin transcript exhibited a notable reduction in the number of photoreceptors by 8 weeks of age,[11] whereas in another study, expression levels as high as 100% over endogenous levels did not cause retinal degenerative changes.[10] This discrepancy may result from the use of a semiquantitative method such as PCR to determine the steady state levels of opsin transcripts.[10,11] Although we determined the amount of the protein rather than the transcript, we find our data more in agreement with the first study, because only approximately 20% overexpression of opsin was sufficient to cause functional deficits and structural abnormalities in ROSs. In this regard, it is worth noting that homozygous *Bouse* A mice, presumably expressing twice as much opsin (>40%), exhibited a more severe retinal degeneration than did their heterozygous counterparts (data not shown). Finally, it is of interest to note that no studies of opsin overexpression have reported a notable increase in the length or width of the ROS, despite the increase in opsin synthesis and the fact that overexpressed opsin is localized to the ROS.[10,11] Nevertheless, careful morphometric analysis will be required to demonstrate conclusively whether or not ROS of mice overexpressing rhodopsin have abnormal dimensions.

The present results indicate that it is difficult to conclude that the degeneration is uniquely related to the particular gene defect that was introduced, without dissection of the deleterious effect induced by overexpression of opsin itself. Moreover, it is possible that a similar situation applies to other models in which a mutant opsin transgene is expressed either in pigs[13,43,51] or rats.[52] With mice, the development of opsin$^{-/-}$ lines[24,25] provides the opportunity to distinguish between these two factors. The properties of a mutant opsin can be evaluated by expression in the opsin$^{-/-}$ background. In certain cases it may be more appropriate to express a transgene in opsin$^{+/-}$ heterozygotes, which express only 50% of the endogenous (wild-type) protein. This is determined by the levels of expression of the mutant transgenic protein. Although other techniques, including knock-in, have the potential to introduce a mutant rhodopsin gene in a manner that allows experimental results to be clearly interpreted, the present study emphasizes the need for the continued development of accurate animal models for human photoreceptor degeneration associated with opsin mutations.

The Degenerative Mechanism

There are several possible mechanisms by which the overexpression of opsin could lead to death of rod photoreceptors. For example, the overproduction of opsin could simply overwhelm the transport machinery, and cell death would be initiated by mislocalized opsin molecules. Although opsin mislocalization has been observed in transgenic mice expressing pig[51] or human[10,11] opsins, electron microscopic immunoanalysis of retinas of *Bouse* A transgenic mice indicate that both endogenous and transgenic opsins were properly localized to the OSs. These results argue against opsin mislocalization as a major cause of cell death in *Bouse* mice.

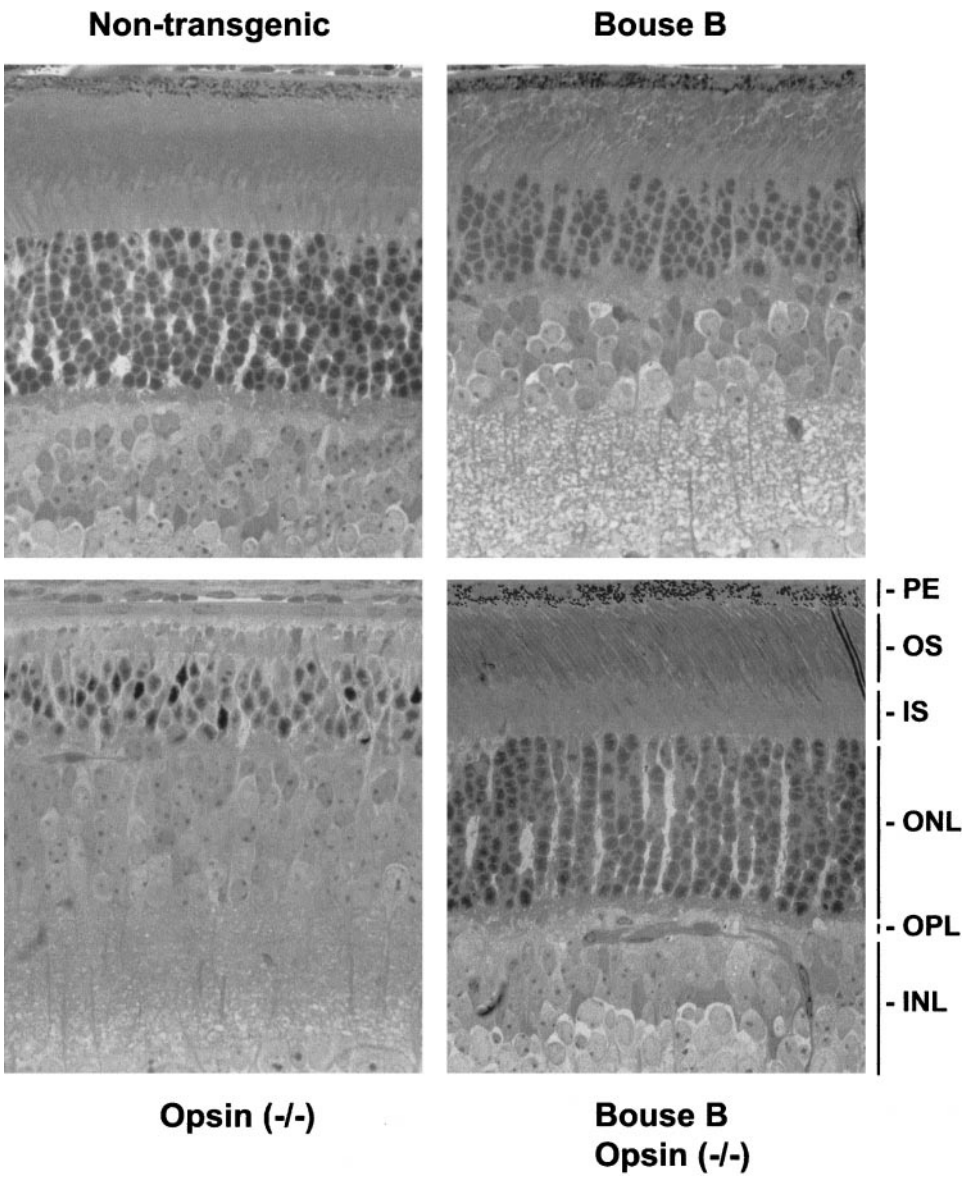

FIGURE 9. Histologic appearance of retinas from cyclic-light–reared *Bouse* B and nontransgenic mice in the wild-type and opsin$^{-/-}$ backgrounds at P30. Abbreviations are as in Figure 3.

The relationship between opsin levels and the amount of 11-*cis* retinal in the retina was examined at P15, an age when OS has been elaborated and degeneration is minimal. In *Bouse* A mice, for which the overexpression of opsin was on average 23%, the amount of 11-*cis* retinal per unit density of ONL nuclei exceeded the average for nontransgenic mice by 26% (Table 1, right column). Relative amounts of opsin were normalized to the amount of peripherin/rds in the analyzed sample because its levels at P10 were comparable in both *Bouse* transgenic and nontransgenic retinas as determined by western analyses (data not shown). Because at P15 retinal degeneration in *Bouse* C is already under way (data not shown), peripherin/rds was used to account for the loss of OS assuming that opsin and peripherin/rds disappear at the same rate with the reduction in the OS. The values for relative opsin level are effectively scaled to the number of photoreceptors present, and the level of opsin overexpression may be compared with the observed increase in 11-*cis* retinal in *Bouse* A mice. The results suggest that in *Bouse* A opsin overexpression leads to increase of 11-*cis* retinal sufficient to match the chromophore requirement of the 23% opsin overexpression. There would appear, however, to be a limit to such an induced increase in 11-*cis* retinal level. In the higher expressing *Bouse* B and C, a substantial percentage of opsin molecules have no 11-*cis* retinal chromophore. It has been suggested that free opsin arising in vitamin A deprivation, as well as some mutant forms of opsin that cannot bind 11-*cis* retinal, can excite the phototransduction cascade.[53] It would be of interest in future studies to examine the effect in *Bouse* B and *Bouse* C mice of systemic vitamin A administration, a treatment that has been found in other studies of transgenic mice[54] and human trials[55] to promote recovery of visual sensitivity.

There are several other means through which overexpression of opsin could lead to cell death. For example, because some fraction of the overproduced opsin is coupled to the chromophore, the number of photobleachable rhodopsin molecules is increased. As a result, a given amount of light falling on the retina would be expected to activate relatively more rhodopsin molecules in *Bouse* retinas than it does in the normal retina. If there is a limited supply of proteins that are involved in deactivating the phototransduction cascade, the photoactivated rhodopsin may have a longer life—that is, the effect can be likened to prolonged light exposure.

Because dark rearing of *Bouse* A mice did not restore their ERGs to those of their normal counterparts, there must be another mechanism besides the increased amount of total rhodopsin that contributes to the cell death. Opsin constitutes 80% to 90% of the OS proteins,[56,57] and because 10% of the OS

is regenerated each day[58] the cell must resynthesize 10% of total opsin daily, as well as all the other proteins that are required for the genesis of the OS. These other proteins include peripherin/rds, rom-1, the phototransduction cascade members as well as the proteins involved in packaging, transport and OS assembly. Because it appears that the vast majority of the available opsin is shipped to the OSs of *Bouse* mice, the increased synthesis of opsin presumably is also associated with an increased synthesis of other needed proteins. As a result, in *Bouse* mice, it is feasible that the photoreceptor cell is functioning at the threshold of its maximum translational capacity. The net result is a situation that is likely to be unsustainable and may ultimately lead to cell death.

It is interesting to note that the same situation does not appear to apply to cone photoreceptors. Shaaban et al.[59] studied transgenic mice in which the human long-wavelength cone opsin gene was expressed in cones of transgenic mice using the human red-green cone opsin promoter. These mice exhibited no evidence of cone photoreceptor degeneration, even when the transgenic cone opsin was expressed at rod opsin levels that are known to compromise rod photoreceptors.[10,11] This may be due to the considerably faster regeneration of the photobleached cone pigment when compared with rhodopsin.[60–62] The explanation for this fundamental difference between rod and cone photoreceptors may provide important insights into the photoreceptor degeneration induced by opsin overexpression.

Clinical Implications

The results described here have implications for the understanding of photoreceptor degeneration, particularly in retinitis pigmentosa. Although much effort has been devoted to the identification of point mutations in the coding regions of the opsin gene, it is possible that some forms of retinitis pigmentosa may be due to an abnormally high level of rhodopsin (or opsin) expression. To evaluate this possibility, it is important to understand the regulatory mechanism that controls the rate of opsin gene expression. In this regard it is interesting to note that mutations in *Crx*, a regulatory element for opsin expression, are linked to retinitis pigmentosa.[63–65] It is possible that a dominant positive mutation in *crx* could lead to rhodopsin overexpression, thus causing a retinal degenerative disorder. If this is the case, the *Bouse* mouse could provide a useful model in which to conduct treatment trials, through pharmacologic intervention, gene therapy, or other means.

In conclusion, the present results confirm that rod photoreceptor degeneration can be induced by overexpression of a normal opsin gene, a factor that should be considered when evaluating studies of mice expressing a mutant opsin transgene. These results also indicate that precise control of opsin expression is of critical importance in maintaining viable photoreceptors. As a consequence, these findings underscore the importance of completely identifying genes that regulate rhodopsin expression. They further indicate that identification of these genes is a potentially fruitful avenue for the identification of gene defects that may underlie retinitis pigmentosa and other retinal disorders.

Acknowledgments

The authors thank Harris Ripps for helpful comments on the manuscript; Jiang Yu, Chi-yen Miller, Laura Bucher, and Shihong Li for technical help; Robert S. Molday and Gabriel Travis for providing the antibodies used in this study; and Nancy Mangini for providing some of the bovine ROS preparations used.

References

1. Rattner A, Sun H, Nathans J. Molecular genetics of human retinal disease. *Ann Rev Genet.* 1999;33:89–131.
2. Berson EL. Retinitis pigmentosa: The Friedenwald Lecture. *Invest Ophthalmol Vis Sci.* 1993;34:1659–1676.
3. Heckenlively JR. Autosomal dominant retinitis pigmentosa. *Retinitis Pigmentosa.* Philadelphia: JB Lippincott; 1988:125–149.
4. Humphries P. Hereditary retinopathies: insight into a complex genetic etiology. *Br J Ophthalmol.* 1993;77:469–470.
5. Pagon RA. Retinitis pigmentosa. *Surv Ophthalmol.* 1988;33:137–177.
6. Chen J, Makino CL, Peachey NS, Baylor DA, Simon MI. Mechanism of rhodopsin inactivation in vivo as revealed by COOH-terminal truncation mutant. *Science.* 1995;267:374–377.
7. Gryczan CW, Kuszak JR, Novak L, Peachey NS, Goto Y, Naash MI. A transgenic mouse model for autosomal dominant retinitis pigmentosa caused by a three base pair deletion in codon 255/256 of the opsin gene [ARVO Abstract]. *Invest Ophthalmol Vis Sci.* 1995; 36:**S**423. Abstract nr 1941.
8. Naash MI, Hollyfield JG, Al-Ubaidi MR, Baehr W. Simulation of human autosomal dominant retinitis pigmentosa in transgenic mice expressing a mutated murine opsin gene. *Proc Natl Acad Sci USA.* 1993;90:5499–5503.
9. Naash MI, Al-Ubaidi MR, Hollyfield JG, Baehr W. Simulation of autosomal dominant retinitis pigmentosa in transgenic mice. In: Hollyfield JG, Anderson RE, LaVail MM *Retinal Degeneration: Clinical and Laboratory Applications*. New York: Plenum; 1993: 201–210.
10. Olsson JE, Gordon JW, Pawlyk BS, et al. Transgenic mice with a rhodopsin mutation (Pro23His): a mouse model of autosomal dominant retinitis pigmentosa. *Neuron.* 1992;9:815–830.
11. Sung C-H, Makino C, Baylor D, Nathans J. A rhodopsin gene mutation responsible for autosomal dominant retinitis pigmentosa results in a protein that is defective in localization to the photoreceptor outer segment. *J Neurosci.* 1994;14:5818–5833.
12. Zozulya SA, Gurevich VV, Zvyaga TA, et al. Functional expression in vitro of bovine visual rhodopsin. *Protein Eng.* 1990;3:453–458.
13. Huang PC, Gaitan AE, Hao Y, Petters RM, Wong F. Cellular interactions implicated in the mechanism of photoreceptor degeneration in transgenic mice expressing a mutant rhodopsin gene. *Proc Natl Acad Sci USA.* 1993;90:8484–8488.
14. Chen J, Woodford, B, Jiang, H, Nakayama T, Simon MI. Expression of a c-terminal truncated rhodopsin gene leads to retinal degeneration in transgenic mice [ARVO Abstract]. *Invest Ophthalmol Vis Sci*. 1993;34:**S**768. Abstract nr 333.
15. Hicks D, Molday RS. Differential immunogold-dextran labeling of bovine and frog rod and cone cells using monoclonal antibodies against bovine rhodopsin. *Exp Eye Res.* 1986;42:55–71.
16. Hodges RS, Heaton RJ, Robert Parker JM, Molday L, Molday RS. Antigen-antibody interaction: synthetic peptides define linear antigenic determinants recognized by monoclonal antibodies directed to the cytoplasmic carboxyl terminus of rhodopsin. *J Biol Chem.* 1988;263:11768–11775.
17. Al-Ubaidi MR, Pittler SJ, Champagne MS, Triantafyllos JT, McGinnis JF, Baehr W. Mouse opsin: gene structure and molecular basis of multiple transcripts. *J Biol Chem.* 1990;265:20563–20569.
18. Deretic D, Puleo–Scheppke B, Trippe C. Cytoplasmic domain of rhodopsin is essential for post-Golgi vesicle formation in a retinal cell-free system. *J Biol Chem.* 1996;271:2279–2286.
19. Hogan B, Costantini F, Lacy E. *Manipulating The Mouse Embryo: A Laboratory Manual*. Cold Spring Harbor, New York: Cold Spring Harbor Laboratory; 1986.
20. Chen S, Evans GA. A simple screening method for transgenic mice using the polymerase chain reaction. *Biotechniques.* 1990;8: 32–35.
21. Quiambao AB, Peachey NS, Mangini NJ, Rohlich P, Hollyfield JG, Al-Ubaidi MR. A 221-bp fragment of the mouse opsin promoter directs expression specifically to the rod photoreceptors of transgenic mice. *Vis Neurosci.* 1997;14:617–625.
22. Xu X, Quiambao AB, Roveri L, et al. Degeneration of cone photoreceptors induced by expression of the *Mas1* proto-oncogene. *Exp Neurol.* 2000;163:207–219.
23. O'Brien J, Ripps H, Al-Ubaidi MR. Molecular cloning of a rod opsin cDNA from the skate retina. *Gene.* 1997;193:141–150.
24. Lem J, Krasnoperova NV, Calvert PD, et al. Morphological, physiological and biochemical changes in rhodopsin knockout mice. *Proc Natl Acad Sci USA.* 1999;96:736–741.

25. Humphries MM, Rancourt D, Farrar GJ, et al. Retinopathy induced in mice by targeted disruption of the rhodopsin gene. *Nat Genet.* 1997;15:216–219.
26. Peachey NS, Goto Y, Al-Ubaidi MR, Naash MI. Properties of the mouse cone-mediated electroretinogram during light adaptation. *Neurosci Lett.* 1993;162:9–11.
27. Al-Ubaidi MR, Hollyfield JG, Overbeek PA, Baehr W. Photoreceptor degeneration induced by the expression of simian virus 40 large tumor antigen in the retina of transgenic mice. *Proc Natl Acad Sci USA.* 1992;89:1194–1198.
28. Moore KL, Graham MA, Barr ML. The detection of chromosomal sex in hermaphrodites from a skin biopsy. *Surg Gynecol Obstet.* 1953;96:641–648.
29. Moore KL, Graham MA, Barr ML. Nuclear morphology, according to sex, in human tissues. *Acta Anat.* 1954;21:197–208.
30. Erickson PA, Lewis GP, Fisher SK. Post-embedding immunocytochemical techniques for light and electron microscopy. *Methods Cell Biol.* 1993;37:283–310.
31. Laemmli UK. Cleavage of structural proteins during assembly of the head of bacteriophage T4. *Nature.* 1970;227:680–685.
32. Towbin H, Staehelin T, Gordon J. Electrophoretic transfer of proteins from polyacrylamide gels to nitrocellulose sheets: procedure and some applications. *Proc Natl Acad Sci USA.* 1979;76:4350–4354.
33. Kedzierski W, Weng J, Travis GH. Analysis of the rds/peripherionrom1 complex in transgenic photoreceptors that express a chimeric protein. *J Biol Chem.* 1999;274:29181–29187.
34. Papermaster DS. Preparation of retinal rod outer segments. *Methods Enzymol.* 1982;81:48–52.
35. Litman B. Purification of rhodopsin by concanavalin A affinity chromatography. *Methods Enzymol.* 1982;81:150–160.
36. Qtaishat NM, Okajima TIL, Li S, Naash MI, Pepperberg DR. Retinoid kinetics in eye tissues of VPP transgenic mice and their normal littermates. *Invest Ophthalmol Vis Sci.* 1999;40:1040–1049.
37. Suzuki T, Fujita Y, Noda Y, Miyata S. A simple procedure for the extraction of the native chromophore of visual pigments: the formaldehyde method. *Vision Res.* 1986;26:425–429.
38. Suzuki T, Maeda Y, Toh Y, Eguchi E. Retinyl and 3-dehydroretinyl esters in the crayfish retina. *Vision Res.* 1988;28:1061–1070.
39. Okajima T-IL, Pepperberg DR. Retinol kinetics in the isolated retina determined by retinoid extraction and HPLC. *Exp Eye Res.* 1997;65:331–340.
40. Robson JG, Frishman LJ. Response linearity and kinetics of the cat retina: the bipolar cell component of the dark-adapted electroretinogram. *Vis Neurosci.* 1996;12:837–850.
41. Lamb TD. Gain and kinetics of activation in the G-protein cascade of phototransduction. *Proc Natl Acad Sci USA.* 1996;93:566–570.
42. Goto Y, Peachey NS, Ripps H, Naash MI. Functional abnormalities in transgenic mice expressing a mutant rhodopsin gene. *Invest Ophthalmol Vis Sci.* 1995;36:62–71.
43. Petters RM, Alexander CA, Wells EB, et al. Genetically engineered large animal model for studying cone photoreceptor survival and degeneration in retinitis pigmentosa. *Nat Biotech.* 1997;15:965–970.
44. Peachey NS, Fishman GA, Derlacki DJ, Alexander KR. Rod and cone dysfunction in carriers of X-linked retinitis pigmentosa. *Ophthalmology.* 1988;95:677–685.
45. Birch DG, Anderson JL, Fish GE. Yearly rates of rod and cone functional loss in retinitis pigmentosa and cone-rod dystrophy. *Ophthalmology.* 1999;106:258–268.
46. Wong F. Visual pigments, blue cone monochromasy, and retinitis pigmentosa. *Arch Ophthalmol.* 1990;108:935–936.
47. Sandberg MA, Berson EL. Blue and green cone mechanisms in retinitis pigmentosa. *Invest Ophthalmol Vis Sci.* 1977;16:149–157.
48. Hood DC, Birch DG. Abnormalities of the retinal cone system in retinitis pigmentosa. *Vision Res.* 1996;36:1699–1709.
49. Travis GH, Sutcliffe JG, Bok D. The *retinal degeneration slow* (*rds*) gene product is a photoreceptor disc membrane-associated glycoprotein. *Neuron.* 1991;6:61–70.
50. Travis GH, Bok D. A molecular characterization of the *retinal degeneration slow* (*rds*) mouse mutation. In: Hollyfield JG, Anderson RE, LaVail MM, eds. *Retinal Degeneration: Clinical and Laboratory Applications.* New York: Plenum; 1993:219–230.
51. Wong F. Creating transgenic mouse models of photoreceptor degeneration caused by mutations in the rhodopsin gene. In: Hollyfield JG, Anderson RE, LaVail MM, eds. *Retinal Degeneration: Clinical and Laboratory Applications.* New York: Plenum; 1993: 211–217.
52. Steinberg RH, Flannery JG, Naash MI, et al. Transgenic rat models of inherited retinal degeneration caused by mutant opsin genes [ARVO Abstract]. *Invest Ophthalmol Vis Sci.* 1996;37(3):**S**698. Abstract nr 3190.
53. Fain GL, Lisman JE. Photoreceptor degeneration in vitamin A deprivation and retinitis pigmentosa: the equivalent light hypothesis. *Exp Eye Res.* 1993;57:335–340.
54. Li T, Sandberg MA, Pawlyk BS, et al. Effect of vitamin A supplementation on rhodopsin mutants threonine-17-methionine and proline-347-serine in transgenic mice and in cell cultures. *Proc Natl Acad Sci USA.* 1998;95:11933–11938.
55. Berson EL, Rosner B, Sandberg MA, et al. A randomized trial of vitamin A and vitamin E supplementation for retinitis pigmentosa. *Arch Ophthalmol.* 1993;111:761–772.
56. Molday RS, Molday LL. Differences in the protein composition of bovine retinal rod outer segment disk and plasma membranes isolated by a ricin-gold-dextran density perturbation method. *J Cell Biol.* 1987;105:2589–2601.
57. Papermaster DS, Dreyer WJ. Rhodopsin content in the outer segment membranes of bovine and frog retinal rods. *Biochemistry.* 1974;13:2438–2444.
58. Young RW. Visual cells and the concept of renewal. *Invest Ophthalmol Vis Sci.* 1976;15:700–725.
59. Shaaban SA, Crognale MA, Calderone JB, Huang J, Jacobs GH, Deeb SS. Transgenic mice expressing a functional human photopigment. *Invest Ophthalmol Vis Sci.* 1998;39:1036–1043.
60. Ripps H, Weale RA. Rhodopsin regeneration in man. *Nature.* 1969;222:775–777.
61. Alpern M, Maaseidvaag F, Ohba N. The kinetics of cone visual pigments in man. *Vision Res.* 1971;11:539–549.
62. Hollins M, Alpern M. Dark adaptation and visual pigment regeneration in human cones. *J Gen Physiol.* 1973;62:430–447.
63. Swaroop A, Wang QL, Wu W, et al. Leber congenital amaurosis caused by a homozygous mutation (R90W) in the homeodomain of retinal transcription factor CRX: direct evidence for the involvement of CRX in the development of photoreceptor function. *Hum Mol Genet.* 1999;8:299–305.
64. Jacobson SG, Cideciyan AV, Huang Y, et al. Retinal degeneration with truncation mutations in the cone–rod homeobox (*CRX*) gene. *Invest Ophthalmol Vis Sci.* 1998;39:2417–2426.
65. Sohocki MM, Sullivan LS, Mintz-Hittner HA, et al. A range of clinical phenotypes associated with mutations in CRX, a photoreceptor transcription-factor gene. *Am J Hum Genet.* 1998;63:1307–1315.